Application of Geospatial Machine Learning Model for Above Ground Biomass Estimation in Mangroves Forest

TingTing Han* and Poonperm Vardhanabindu

Faculty of Environment and Resource Studies, Mahidol University, Nakhon Pathom, Thailand
*Corresponding author, E-mail: tingting.mahidol@gmail.com

Abstract

The dangers and difficulties that occur during ground-based studies of mangrove forests present an opportunity to develop cheap, accurate, and easy-to-use remote sensing methods. In this study, an Unmanned Aerial Vehicle (UAV) uses Very High Resolution (VHR) imagery to determine the carbon emissions stored as Above-Ground Biomass (AGB) in a mangrove forest in Klong Khon, Thailand. Four 100 m^2 plots were used to develop a model that uses tree height and crown area to estimate Diameter at Brest Height (DBH) (Deviance = 76.0%). The UAV uses Structure from Motion (SfM) to determine mangrove height and crown area to then model DBH. Two Variable Window Filtering (VWF) algorithms were applied to UAV imagery to detect treetops and crown delineation. Power regression and lower limit VWF models were developed using the relationship between ground measured tree height and crown diameter. Ground- and UAV-based dendrometric parameters were compared with ground-based measurements to determine their accuracy.

Keywords**:** *Above ground biomass, Mangrove forest, Machine learning, UAVs, Cloud point, Digital model*

1. Introduction

The warming of the globe has led to increasing interest in the world's carbon stocks (Asner, 2009; Dangal et al., 2017; Smith et al., 2019). Mangroves, salt marshes, and seagrasses are all important ecosystems that are defined as "blue carbon." Blue carbon ecosystems sequester more carbon than terrestrial forests and have been reported to lock carbon away for millennia (McKee et al., 2007; Mcleod et al., 2011). The carbon sequestered in these environments is divided into living or dead Above-Ground Biomass (AGB) and Below-Ground Biomass (BGB), as well as carbon stored within the soil (Howard et al., 2014). Methods for determining AGB are well established, cost-effective, and easier to carry out than methods for surveying BGB (Ravindranath and Ostwald, 2008). Mangroves store more carbon in their AGB than salt marshes or seagrasses (Bulmer et al., 2020), and have been widely researched as a consequence (Mitra et al., 2011; Ray et al., 2011; Van Vinh et al., 2019).

The ability of mangroves to effectively sequester carbon means that that they are well recognized amongst international initiatives as a mechanism to alleviate the stress caused by climate change. These include the United Nations Framework Convention on Climate Change (UNFCCC) Reducing Emissions from Deforestation and Forest Degradation (REDD+) scheme and the 2013 Coastal Wetlands Supplement to the 2006 Intergovernmental Panel on Climate Change (IPCC) Guidelines for National Greenhouse Gas Inventories (Hiraishi et al., 2014). There are also numerous carbon financing schemes dispersed around the globe. Mikoko Pamoja and the Blue Ventures Organisation both promote sustainable development whilst discouraging mangrove degradation and deforestation (Jones et al., 2016; Wylie et al., 2016). These schemes lend themselves to accurate carbon stock estimations as this improves carbon credit trading as well as optimizing management (Cairns and Lasserre, 2004). A caveat to many mangrove ecosystem studies is that forests exhibit spatial heterogeneity as well as variety between sites (Thompson et al., 2014). As a result, new allometric equations need to be developed for each mangrove study site (Van Vinh et al., 2019). Unfortunately, this means that many carbon storage estimates covering large areas are inaccurate (Ouyang and Lee, 2020).

Mangrove carbon stock estimations have traditionally been carried out using ground-based measurements (Ray et al., 2011; Alongi et al., 2016; Bulmer et al., 2016). These measurements catalog dendrometric parameters such as tree height, crown area, and diameter at breast height (DBH) (Owers et al., 2018a). These parameters can be used to determine AGB, which can then be converted into the equivalent

carbon emissions (CO_2). For this to be possible, extensive measurements need to be made across a large study site to allow for an accurate representation of the forest (Kauffman and Donato, 2012), which presents a number of problems due to the difficulty of studying mangrove forests. The remoteness and density of mangrove forests make them difficult to access with fieldwork being expensive, time-consuming, and dangerous (Friess, 2016).

Remote sensing as a method to estimate carbon in mangroves has been increasingly used as technology has advanced and practices have been refined (Fatoyinbo and Simard, 2013; Wicaksono, 2017; Hickey et al., 2018). Passive methods of remote sensing (Landsat) produce data that can estimate carbon stocks across large areas (Aslan et al., 2016). However, the coarse-scale of these datasets means that spatial heterogeneity is difficult to detect (Owers et al., 2016). More detailed active remote sensing methods have been utilized such as very high resolution (VHR) imagery and terrestrial laser scanning (TLS), which both allow for detailed sub-meter measurements (Neukermans et al., 2008; Owers et al., 2018b). The greater resolution obtained from these methods allows for more accurate site-specific carbon stock estimations (Komiyama et al., 2005). While these datasets are useful, they are not easily accessible to the relevant communities as mangroves mostly occur in developing countries (Osland et al., 2017). The need for a remote sensing method that is cheap, accessible, easy to deploy, and can be used to collect VHR data to study mangroves is evident. These issues look to be solved by the increasing use of Unmanned Aerial Vehicles (UAVs) in the scientific literature (Lin et al., 2010; Turner et al., 2016). The highly detailed and comparatively cheap site-specific data collected by UAVs means that they have been successfully used in terrain modeling, agriculture, and studying dendrometric parameters (Gómez-Candón et al., 2014; Gonçalves and Henriques, 2015; Torresan et al., 2017).

In this study, a UAV is used to create a model that can determine the dendrometric parameters within a mangrove forest located in the Upper Thai Gulf, Thailand. Ground-based measurements were compared with UAV-based measurements to assess the comparability of dendrometric parameters, which will allow carbon stock estimates to be developed for the above-ground carbon emissions of the forest.

2. Objectives

1) To develop a geospatial VWF model to got the Mangrove forest crown diameter and canopy size
2) To calculate the above-ground carbon stock of mangrove forests
3) To compare the geospatial VWF method with the ground measurement method

3. Materials and Methods

3.1 Study site

The study site is located along the North-West coast of the Upper Thai Gulf in Klong Khon's mangrove forest in Samut Songkram (13°19'N, 99°58'E) (Figure 1). The forest is dominated by *Avicennia officinalis* (91%), but *Rhizophora apiculata* (6%) and *A. alba* (3%) are also present. Man-made canals border the study site, which increases the influx of nutrients to the forest during tidal inundation, resulting in highly productive conditions (Ewel *et al*., 1998). The height and density of *Avicennia* canopies mean that very few understory plants are able to grow (Kitamura *et al*., 1997). To determine the dendrometric parameters of the mangroves present at Klong Khon, ground-based measurements were taken of all trees within four 10 x 10 m plots (400 m^2).

Figure 1 A world map shows the location of the Upper Thai Gulf. The location of Klong Khon is depicted by the black dot (left) and the area captured within the UAV imagery (right)

3.2 Ground-based measurements

The four plots were taken along a transect between the landward and seaward sides of the forest (May 7th, 2019). The first plot was drawn out at the start of the transect and the remaining three plots were taken at random intervals. The dendrometric parameters recorded for each tree include the height that was measured using a smartphone app (Smart Measure), the stem diameter at breast height (DBH) (1.3 m), and the crown diameter (Kauffman and Donato, 2012). The crown area of each tree was determined using the equation for calculating the area of an oval (Equation A1). Any trees with a height that did not surpass 1.3 m were not recorded and any trees with a split stem below 1.3 m were recorded as separate trees (Fu and Wu, 2011).

3.3 Data processing of Ground-based measurements

Tree height, crown area, and diameter at breast height (DBH) were all transformed using the natural logarithm and normally distributed. The use of all 32 trees in the four plots allowed accurate dendrometric relationships to be determined (Kauffman and Donato, 2012). Tree height and crown area were both significantly positively correlated with DBH ($|r| = 0.727$, $p < 0.01$; $|r| = 0.790$, $p < 0.01$, respectively ($df = 30$)). General linear models (GLMs) were created to predict DBH using tree height and crown area. The three models were evaluated using model statistics (Deviance (%), AIC, and Variance Inflation Factors [VIFs]) to determine, which was the most powerful model at predicting DBH. The Root Mean Square Error (RMSE) was used to determine the accuracy of modeled DBH values. Analyses carried out and models created were done so in R Statistical Software (v 3.6.2; http://www.r-project.org/).

3.4 UAV data collection and development

The UAV used in the study was a DJI Phantom 4 pro with a 1-inch 20MP sensor and a DJI Mavic Air mounted with a 12MP sensor. A flight plan was developed using the PIX4D mapper photogrammetry software to ensure uniform coverage to the study site. The UAV traveled at the middle-speed setting and varied in height between 50-70 meters. Images were taken with the camera at a 90° angle with an 80% overlap of images and a resolution of 5-7 cm/pixel, which allows the study site's structure to be recreated using Structure from Motion (SfM). In total, 53 images were captured and uploaded to Pix4D mapper (v4.5.6; https://www.pix4d.com/). The software identifies key points in overlapping images and ties them together. A dense 3D point cloud was generated with a mean density of 165 points/m^3 (Figure A1). The point cloud was edited in CloudCompare (v2.6.2; http://www.danielgm.net/cc/release/) where unwanted noise and anomalous points were removed.

3.5 UAV data analysis

Point cloud data manipulation was done in R using the lidR package: v3.0.4 (Roussel et al., 2018) to a resolution of 5 cm/pixel. A cloth simulation was used on a reversed point cloud to create a digital terrain model (DTM) (Zhang et al., 2016). The height of the canopy was then normalized by using a k-nearest neighbor approach with an inverse distance weighting (KNNIDW). A local maximum filter uses an algorithm to create a diameter (window) around each point within the point cloud. The highest points within each window are then defined as treetops (Wang et al., 2004). The diameter of the filter's window is critical for correctly determining the treetops of the canopy. Variable Window Filtering (VWF) uses tree height to assign a window size to each point for accurate tree segmentation. Using the principle that as trees get taller their crowns get larger, a VWF algorithm can be created. VWF has been used successfully to delineate trees in mangrove forests (Wannasiri et al, 2013; Navarro et al., 2020). In this study, two VWF models were developed and their accuracy was compared with ground measurements. The first of these functions uses the best fitting regression model, which relates tree height to crown diameter (Popescu and Wynne, 2004). The power regression VWF model was the strongest (R^2 = 0.302) and was used as the VWF algorithm (Figure 2a). Since this regression model explained little variance (Hair et al., 2011), it suggests that in this forest, tree height does not dictate crown diameter. To create a robust VWF algorithm for these conditions, a 'lower limit' function was created that allows the greatest window size to be created whilst including the parameters of all ground-based measurements (Figure 2b). While the lower limit VWF model will falsely identify treetops, it is far less likely to miss treetops than the regression model.

Table 1 The type of regression used to determine the relationship between tree height and crown diameter. The equation and R^2 values are displayed. The power regression was used as it had the greatest R^2 value

Regression	**Equation**	**R^2**
Exponential	Crown Diameter = $3.3193e^{0.042(\text{Tree Height})}$	0.293
Linear	Crown Diameter = 0.2238(Tree Height) + 3.3498	0.253
Logarithmic	Crown Diameter = 2.3887ln(Tree Height) + 0.4356	0.257
Power*	Crown Diameter = $1.9087(\text{Tree Height})^{0.4513}$	0.302

Once the VWF models have assigned treetops to the canopy, the crowns can then be grown out using a decision tree-based model (Dalponte and Coomes, 2016). Tree height and crown area were then determined for each tree in ArcGIS Pro (V.2.3.3). These values were used to predict the DBH of each tree before determining AGB (Komiyama et al., 1987) (Equation 1). The reported carbon content of mangrove trees varies between a factor of 0.45-0.50 (Twilley et al., 1992; Kauffman and Donato, 2012). This study used a carbon conversion rate of 0.475 before calculating the equivalent CO_2 emissions (Hamilton and Friess, 2018). Standardized area metrics were calculated by removing the canal from the UAV imagery so that AGB and CO_2 emissions represent values of continuous mangrove forest.

3.6 Statistical analysis

A Shapiro-Wilk normality test was used on tree height, crown area, DBH, and individual tree AGB. Since the four variables were non-normally distributed ($p < 0.05$), Wilcoxon Rank-Sum tests were carried out on all variables to assess if ground-based medians significantly differed from the two VWF models (Navarro et al., 2020).

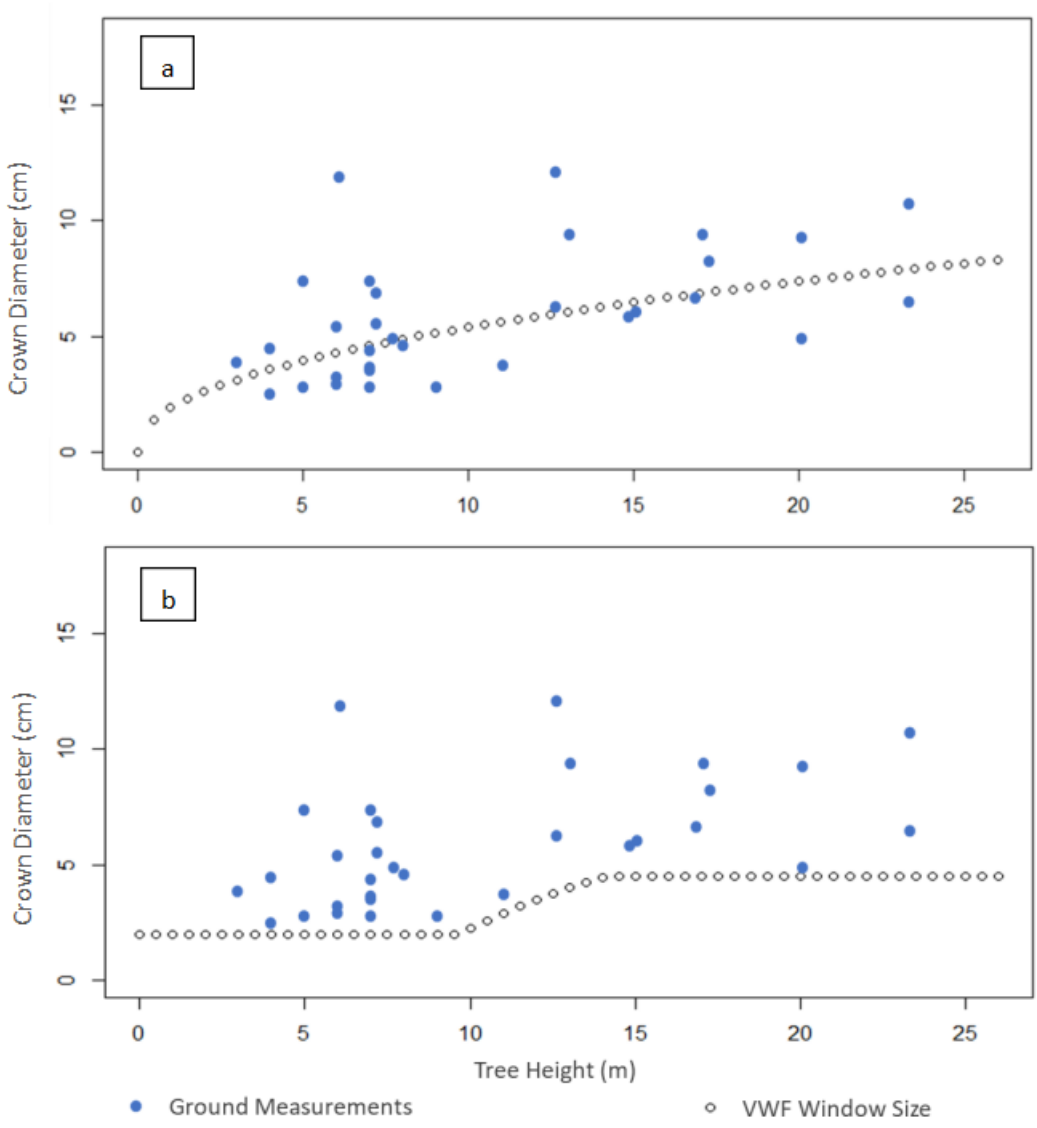

Figure 2 The power regression VWF algorithm (a) and the lower limit VWF algorithm (b) are depicted by white dots at 0.5 m intervals

Table 2 The equations for calculating above-ground biomass in mangroves forest (equation 1).

Tree Stem (kg)	$= 0.05466(D^2H)^{0.945}$	Equation 1
Tree Branch (kg)	$= 0.01579(D^2H)^{0.9124}$	
Tree Leaves (kg)	$= 0.06780(D^2H)^{0.5806}$	
Tree Mass (kg)	= Stem + Branch + Leaves	
D = Diameter at Breast Height, H = (Tree) Height		

4. Results and Discussion

4.1 Results

Tree height and crown area were significantly positively correlated with DBH ($|r| = 0.727$, $p < 0.01$; $|r| = 0.790$, $p < 0.01$, respectively ($df = 30$)) (Figure 3). DBH was most accurately predicted when tree height and crown area were used in the same GLM (Table 3). The tree height and crown area model explained 76.0% of the deviance as well as having the lowest AICc value (= 21.5) and VIFs < 2 (Zuur et al., 2010). The accuracy of this model is greater than either of the other two models as they both exhibit a $\Delta AIC > 7$ (Burnham et al., 2011) (Table 4). Ground-measured DBH values were compared with modeled DBH values and an RMSE of 6.16 cm was calculated.

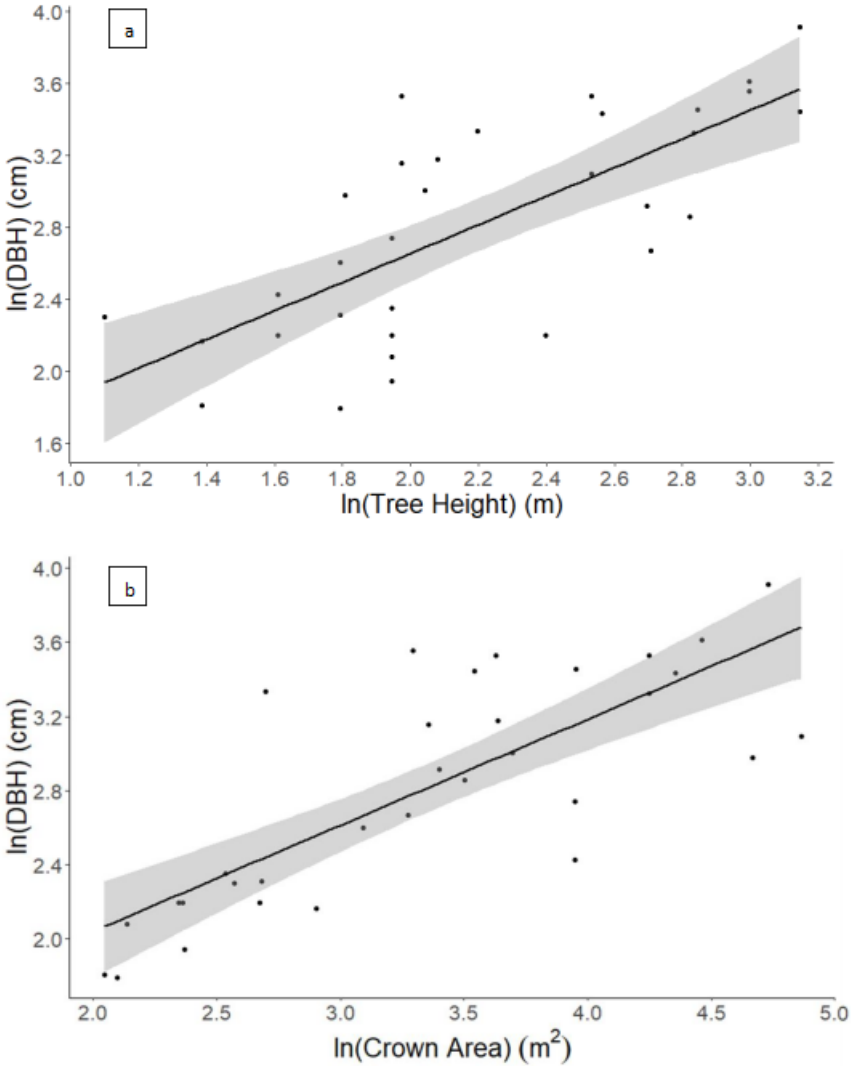

Figure 3 a) The relationship between ground measured ln(Tree Height) and ln(DBH) and b) the relationship between ground measured ln(Crown Area) and ln(DBH)

Table 3 The three GLMs created using ground measured Tree Height and Crown Area along with their equation, Deviance (%), AICc, and ΔAIC. The strongest model used Tree Height and Crown Area.

Model Variables	Equation	Deviance (%)	AICc	ΔAIC
Tree Height and Crown Area	EXP(0.47377ln(Tree Height) + 0.40817ln(Crown Area) + 0.40345)	76.0	21.5	0.0
Tree Height	EXP(0.7962ln(Tree Height) + 1.0616)	52.9	33.3	11.8
Crown Area	EXP(0.57153ln(Crown Area) + 0.89935)	62.4	40.5	19.0

The dendrometric parameters measured via ground measurements and both VWF models are summarized below in Table 4. The canopy cover of the site was 94.4%.

Table 4 Ground-based measurements and the VWF algorithms summary statistics for tree height, crown area, and DBH

Method	Height (m)			Crown Area (m^2)			DBH (cm)		
	Min	Median	Max	Min	Median	Max	Min	Median	Max
In-situ	3.00	7.45	23.2	7.73	29.3	129.4	6.00	18.0	50.0
Lower limit VWF	2.84	12.6*	26.6	2.16	24.8	117.3	4.13	18.2	42.2
Power Regression VWF	2.70	15.4*	26.6	7.58	70.8*	240.5	6.15	30.9*	60.5

Ground- and UAV-based measurements estimated similar minimum tree heights (~3 m). The two VWF models detected a maximum tree height of 26.6 m, which was greater than ground measurements (23.2 m). The median ground measured tree height significantly differed from the median tree heights of the VWF models (Wilcoxon Rank-Sum test, both p-values < 0.01). The greater tree height median measured by both VWF models suggests that the average tree in the forest has a greater height than what was measured through ground surveying.

The lower limit VWF model detected a range in crown area between 2.16 m^2 and 117.3 m^2 as well as a median crown area of 24.8 m^2. While ground-based measurements had slightly larger minimum and maximum crown areas (7.73 – 129.4 m^2), the median did not significantly differ (29.3 m^2, Wilcoxon Rank-Sum test, p = 0.30). The power regression VWF model had a similar minimum crown area (7.58 m^2) to the ground-based measurements, but it measured a much larger maximum crown area (240.5 m^2). In addition, the power regression VWF model measured a median crown area of 70.8 m^2, which did significantly differ from the ground measured crown area median (Wilcoxon Rank-Sum test, p <0.01).

The median AGB per tree from the lower limit VWF model (183.1 kg) did not significantly differ from the median ground measured AGB per tree (141.4 kg, Wilcoxon Rank-Sum test, p = 0.12). The median AGB per tree for the power regression VWF model (578.1 kg) and ground-based measurements significantly differed (Wilcoxon Rank-Sum, p < 0.01).

The number of tree stems, AGB, and CO_2 emissions were standardized to a per hectare metric for comparison between ground- and UAV-based measurements as well as wider literature (Table 5). Ground-based measurements extrapolated a tree stem density of 800 ha^{-1}, which is far larger than the UAV-derived tree stem densities. The lower limit VWF model estimated a tree stem density of 367 ha^{-1} whereas the power

regression VWF model estimated a tree stem density of 143 ha^{-1}. Tree stem density observed by ground measurements was a factor of 2.17x denser than the lower limit VWF model and 5.59x denser than the power regression VWF model.

Ground-based measurements suggest that the AGB of the mangrove forest is 247.3 t ha^{-1}, which is greater than the lower limit VWF model by a factor of 2.46 (100.5 t ha^{-1}) and greater than the power regression VWF model by a factor of 2.57 (96.1 t ha^{-1}). Despite varying dendrometric parameters and tree stem densities presented by the two VWF models, the AGB per hectare values concurs with each other. The CO2 emissions stored as AGB according to ground-based measurements are 430.6 (t ha^{-1}) as opposed to the lower limit and power regression VWF models that report CO_2 storage of 175.0 and 167.4 t ha^{-1}, respectively.

Table 5 Standardised area metrics for ground-based measurements and the two VWF models. Variables include the number of tree stems, Above-Ground Biomass (AGB), and CO2 emissions

Method	Number of tree stems (ha^{-1})	AGB (t ha^{-1})	CO2 emissions (t ha^{-1})
In-situ	800	247.3	430.6
Lower limit VWF	367	100.5	175.0
Power Regression VWF	143	96.1	167.4

4.2 Discussion

Tree height and crown area were significantly correlated with DBH (Yao et al., 2012). The relationship exhibited a strong positive correlation for both tree height ($|r| = 0.727$, $p < 0.01$) and crown area ($|r| = 0.790$, $p < 0.01$). The best model included crown area and tree height (AICc = 21.5 and VIFs < 2) (Table 3). This GLM explained 76.0% of the deviance, which suggests that with accurate extraction of tree height and crown area from UAV data, DBH can be modeled effectively. The findings of this study concur with the findings of Hirata et al., (2014) who also used crown area and tree height to determine allometric relationships.

All methods used in this study were able to detect the smallest trees within the study site. Caveats of previous mangrove studies that use VHR UAV imagery are that trees below the canopy layer can be omitted from analysis (Navarro et al., 2020). However, the dense structure of Avicennia-dominated forests means that there are few trees that reside in the understory (Kitamura et al., 1997). The two VWF models used to analyze UAV data detected a greater maximum tree height than ground-based measurements. As maximum tree height was the same for both VWF models (26.6 m) and only marginally greater than ground measured maximum tree height (23.2 m), it is likely that this discrepancy can be explained by natural variation and tree age (Hickey et al., 2018). The median tree height for both the lower limit (12.6 m) and power regression VWF model (15.4 m) was significantly higher than the median tree height from ground-based measurements (7.45 m, Wilcoxon Rank-Sum, $p < 0.01$). Current software may be limited in determining the height of older, taller, oval/spherical-shaped trees as local maxima can be more difficult to distinguish (Panagiotidis et al., 2017). In addition, high canopy cover (94.4%) (Kaartinen et al., 2012) can lead to difficulty in determining the digital terrain model (DTM) as little ground was exposed for cloth simulation (Wannasiri et al., 2013). Without accurate DTM generation, tree normalization may not reflect true tree heights. Unfortunately, the absence of ground control points in this study means the DTM vertical error could not be calculated (Navarro et al., 2020). Tree height measurements have been accurately reported using VHR UAV imagery. Jones et al., (2020) found a near-perfect regression between ground and UAV measured tree height ($R^2 = 0.98$). As a result, it is possible that overestimation of tree height may be due to human error and limitations of ground surveying methods. Trees >2 m may have their heights underestimated as surveyors cannot accurately determine the highest point of the crown (Larjavaara and Muller-Landau, 2013). This error increases with greater canopy cover as well as increased tree height (Yin and Wang, 2019). The higher median

tree height may be a combination of inaccuracies from ground-based measurements due to difficulty in discerning the highest point of the tree as well as difficulty in determining the DTM.

The power regression VWF model had a significantly larger crown area median (70.8 m^2) than ground-based measurements (29.3 m^2, Wilcoxon Rank-Sum test, $p < 0.01$), which is partially due to the weak relationship between tree height and crown diameter ($R^2 = 0.302$) (Falkowski et al., 2006). The poor R^2 value in this study is partly due to all mangrove species being included in the model as the UAV models do not implement species identification techniques (Yin and Wang, 2019). However, this is unlikely to have had a significant impact as Avicennia species make up 94% of the trees. The power regression VWF model's largest caveat is due to ground surveying methods. As already discussed, differences between tree height estimations are likely due to limitations of ground-based methods. With VWF window sizes being determined by tree height, inaccurate ground-based measurements will affect the model's ability to successfully delineate crowns. Underestimation of ground measured tree heights means that datapoints undergo a positive translation up the x-axis (tree height) to achieve their true height (Figure A2a), meaning that the power regression VWF model assigns a greater window size to treetops. As a result of under-segmentation, there are fewer crowns identified with each crown occupying a larger area (Figure A3). Tree height underestimation increases with taller trees, which leads to proportionately smaller window sizes for the tallest trees (Yin and Wang, 2019), which explains why the minimum tree height between the power regression VWF model and ground-based measurements were comparable (7.58 and 7.73 m^2, respectively), but maximum crown areas were not (240.5 and 129.4 m^2, respectively). The minimum and maximum crown areas for the lower limit VWF model were comparable to the crown areas observed in ground-based studies (24.8-117.3 and 29.3-129.4 m^2, respectively). Furthermore, the median crown areas of the two methods did not significantly differ (Wilcoxon Rank-Sum test, $p = 0.30$). The more conservative approach used by the lower limit VWF model means that even when ground-measured datapoints are positively translated up the x-axis (tree height), the window size is not compromised to the same extent as the power regression VWF model (Figure A2b). While this method does not compromise window size, the nature of the lower limit VWF model means that all windows created are smaller than the ground measured crown diameters. As a result, more false-positive treetops are identified (Figure A4). All crown area summary statistics for the lower limit VWF model are less than ground-based measurements, which suggests over-segmentation of crowns and increased number of tree stems (Table 5).

Unfortunately, without extensive ground surveying, it is impossible to derive the commission error (Wannasiri et al., 2013). Nevertheless, comparability of minimum, median, and maximum crown areas between the lower limit VWF model and ground-based measurements suggests that false positives have not significantly impacted results.

The VWF models both measured tree height medians that were significantly greater than the median ground-measured tree height (Wilcoxon Rank-Sum test, $p < 0.01$). It is hypothesized that ground-measured tree heights were underestimated due to limitations of ground surveying methods when canopy conditions are dense and tall. The power regression VWF model did not accurately predict crown area or DBH (Wilcoxon Rank-Sum test, $p < 0.01$ for both variables). Poor estimates of dendrometric parameters from the power regression VWF model are due to a poor relationship between tree height and crown diameter ($R^2 = 0.302$) as well as dense canopy cover (94.4%) decreasing the ability for crown delineation (Wannasiri, et al., 2013). The minimum and maximum DBH modeled by the lower limit VWF model were smaller than the DBH of ground-based measurements, but they were still comparable. Furthermore, the median DBH from ground-based measurements and the lower limit VWF model do not significantly differ (Wilcoxon Rank-Sum, $p = 0.629$) despite tree height medians significantly differing (Wilcoxon Rank-Sum, $p < 0.01$). It suggests that crown area is more significant than tree height in determining DBH, which is a result of the lower limit VWF model estimating a greater range for the crown area than for tree height (2.16-117.3 m^2 and 2.84-26.6 m, respectively) despite similar equation coefficients (Table 3). Consequently, similar DBH medians are reported by the lower limit VWF model and ground-based measurements.

Ground-based measurements estimated tree stem densities of 800 ha^{-1}, which was greater than the lower limit VWF model (367 ha^{-1}) or the power regression VWF model (143 ha^{-1}) (Table 5). Extrapolated

and interpolated stem densities per hectare can widely vary in their estimates due to the spatial heterogeneity of mangrove forests (Owers et al., 2016). As larger plot sizes cover more land, they are better able to capture this variance. Proisy et al., (2007) carried out ground surveys of varying plot sizes that estimated tree stem densities between 53-15,100 ha^{-1}. Generally, interpolation of larger plots found lower tree stem density, and extrapolation of smaller plots found greater tree stem density. In this study, extrapolation of tree stem density from ground-based measurements may be an overestimate as the plots only represent a 400 m^2 area of forest whereas the UAV study site is approximately 37,600 m^2. While mangrove forests with greater tree stem density have been reported, these forests have smaller, more densely packed trees (Wannasiri et al., 2013; Faridah-Hanum et al., 2014).

It was also estimated from ground-based measurements that the AGB of Klong Khon averaged 247.3 t ha^{-1}. In contrast, the lower limit VWF model determined an AGB of 100.5 t ha^{-1} and the power regression VWF model determined an AGB of 96.1 t ha^{-1}. The power regression VWF model under-segmented the canopy, which resulted in overestimations of dendrometric parameters. While the power regression VWF model only detected 39.0% of the lower limit VWF model treetops, each tree had a far greater AGB, which allowed for comparable AGB estimates per hectare between the two models. The AGB per hectare in this study was greater than what has been reported in other Avicennia-dominated forests (Ray et al., 2011), which is most notably due to larger trees found in this study than other Avicennia forests (Duke, 1991).

The number of tree stems per hectare estimated by the lower limit VWF model was less than ground-based measurements by a factor of 2.17 (Table 5). The lower limit VWF model has overestimated the number of tree stems per hectare, which means that ground-based measurements are greater by a factor of >2.17. The AGB per hectare of the lower limit VWF model was less than ground-based measurements by a factor of 2.46. Standardized ground-based measurements are possibly not representative of the mangrove forests' wider heterogeneity. This hypothesis is posed because the lower limit VWF model's number of stems and AGB per hectare is less than ground measurements by comparable factors (>2.17 – 2.46). The similarity of these factors means that ground-based measurements have overestimated standardized per hectare metrics. It is further supported as the median individual tree AGB does not significantly differ between the lower limit VWF model and ground-based measurements (Wilcoxon Rank-Sum, $p < 0.01$). It can therefore be concluded that standardized ground-based measurements are not representative of the wider mangrove forest and the lower limit VWF model estimated AGB should be used (100.5 t ha^{-1}). The AGB can then be converted into CO_2 emissions, which estimates 175.0 t ha^{-1}. A final caveat is that an allometric equation was not developed for this study (Equation 1). While the equation used was accurately developed from the mangroves of the surrounding area (Komiyama et al., 1987), it is possible that due to forest spatial heterogeneity it does not represent the precise AGB of the study area (Owers et al., 2016). A different allometric equation may result in a very different estimate for CO_2 per hectare as studies have shown that the use of tree height can impede AGB estimates (Komiyama et al., 2005), which is because DBH can vary greatly once the maximum species-specific tree height has been reached (Soares and Schaeffer-Novelli, 2005).

5. Conclusion

While a VWF algorithm following regression is favorable when determining window size, this study shows that when regression is weak ($R^2 = 0.302$), a lower limit VWF algorithm can be used to successfully derive the dendrometric parameters of Klong Khon's mangrove forest. Tree heights were the only dendrometric parameter where medians significantly differed between ground-based measurements and the lower limit VWF model. Despite that, crown area and DBH medians did not significantly differ between ground measurements and the lower limit VWF model. The small number of ground surveyed plots means that forest spatial heterogeneity may not have been captured. Consequently, tree height and derived DBH values from the lower limit VWF were used to determine AGB per hectare within the study site. The amount of CO_2 currently stored as AGB within Klong Khon's mangroves is 175.0 t ha^{-1}. To discern the true accuracy of UAV measured tree height, comprehensive research needs to be conducted to establish a tree height estimation error between UAV- and ground-based measurements. Establishing this error index under varying

canopy cover and tree height conditions will strengthen the ability for VHR UAV imagery to measure tree height and determine AGB.

6. References

Alongi, D., Murdiyarso, D., Fourqurean, J., Kauffman, J., Hutahaean, A., Crooks, S., Lovelock, C., Howard, J., Herr, D., Fortes, M. & Pidgeon, E. (2016). Indonesia's blue carbon: a globally significant and vulnerable sink for seagrass and mangrove carbon. *Wetlands Ecology and Management*, *24* (1), 3-13

Aslan, A., Rahman, A., Warren, M. & Robeson, S. (2016). Mapping spatial distribution and biomass of coastal wetland vegetation in Indonesian Papua by combining active and passive remotely sensed data. *Remote Sensing of Environment*, *183*, 65-81

Asner, G. (2009). Tropical forest carbon assessment: integrating satellite and airborne mapping approaches. *Environmental Research Letters*, *4*(3), 1-11

Bulmer, R., Schwendenmann, L. & Lundquist, C. (2016). Allometric models for estimating aboveground biomass, carbon and nitrogen stocks in temperate Avicennia marina forests. *Wetlands*, 36 (5), 841-848

Bulmer, R., Stephenson, F., Jones, H., Townsend, M., Hillman, J., Schwendenmann, L., & Lundquist, C., (2020). Blue Carbon Stocks and Cross-Habitat Subsidies. *Frontiers in Marine Science*, *7* (380), 1-9

Burnham, K., Anderson, D., & Huyvaert, K. (2011). AIC model selection and multimodel inference in behavioral ecology: some background, observations, and comparisons. *Behavioral ecology and sociobiology*, *65*(1), 23-35

Cairns, R., & Lasserre, P. (2004). Reinforcing economic incentives for carbon credits for forests. *Forest Policy and Economics*, *6*(3-4), 321-328

Dalponte, M., & Coomes, D. (2016). Tree-centric mapping of forest carbon density from airborne laser scanning and hyperspectral data. *Methods in ecology and evolution*, *7*(10), 1236-1245

Dangal, S., Das, A., & Paudel, S. (2017). Effectiveness of management interventions on forest carbon stock in planted forests in Nepal. *Journal of environmental management*, *196*, 511-517.

Duke, N., (1991). A systematic revision of the mangrove genus *Avicennia* (Avicenniaceae) in Australasia. *Australian Systematic Botany*, *4*(2), 299-324.

Ewel, K., Twilley, R., & Ong, J. (1998). Different kinds of mangrove forests provide different goods and services. *Global Ecology & Biogeography Letters*, *7*(1), 83-94.

Falkowski, M., Smith, A., Hudak, A., Gessler, P., Vierling, L., & Crookston, N. (2006). Automated estimation of individual conifer tree height and crown diameter via two- dimensional spatial wavelet analysis of lidar data. *Canadian Journal of Remote Sensing*, *32*(2), 153-161.

Faridah-Hanum, I., Latiff, A., Hakeem, K. R., & Ozturk, M. (2014). Mangrove forests in Thailand. In: Pumijumnong, N., ed., *Mangrove Ecosystems of Asia*, 1st ed. New York: Springer, 61- 79.

Fatoyinbo, T., & Simard, M. (2013). Height and biomass of mangroves in Africa from ICESat/GLAS and SRTM. *International Journal of Remote Sensing*, *34*(2), 668-681.

Friess, D. (2016). Ecosystem services and disservices of mangrove forests: insights from historical colonial observations. *Forests*, *7*(9), 183.

Fu, W., & Wu, Y. (2011). Estimation of aboveground biomass of different mangrove trees based on crown diameter and tree height. *Procedia Environmental Sciences*, *10*, 2189- 2194.

Gómez-Candón, D., De Castro, A., & López-Granados, F. (2014). Assessing the accuracy of mosaics from unmanned aerial vehicle (UAV) imagery for precision agriculture purposes in wheat. *Precision Agriculture*, *15*(1), 44-56.

Gonçalves, J., & Henriques, R. (2015). UAV photogrammetry for topographic monitoring of coastal areas. *ISPRS Journal of Photogrammetry and Remote Sensing*, *104*, 101-111.

Hair, J., Ringle, C., & Sarstedt, M., (2011). PLS-SEM: Indeed a silver bullet. *Journal of Marketing theory and Practice*, *19*(2), 139-152.

Hamilton, S., & Friess, D. (2018). Global carbon stocks and potential emissions due to mangrove deforestation from 2000 to 2012. *Nature Climate Change*, *8*(3), 240-244.

Hickey, S., Callow, N., Phinn, S., Lovelock, C., & Duarte, C., (2018). Spatial complexities in aboveground carbon stocks of a semi-arid mangrove community: A remote sensing height- biomass-carbon approach. *Estuarine, Coastal and Shelf Science, 200*, 194-201.

Hiraishi, T., Krug, T., Tanabe, K., Srivastava, N., Baasansuren, J., Fukuda, M., & Troxler, T. (2014). *2013 supplement to the 2006 IPCC guidelines for national greenhouse gas inventories: Wetlands*. IPCC: Geneva

Hirata, Y., Tabuchi, R., Patanaponpaiboon, P., Poungparn, S., Yoneda, R., & Fujioka, Y. (2014). Estimation of aboveground biomass in mangrove forests using high-resolution satellite data. *Journal of Forest Research, 19* (1), 34-41

Howard, J., Hoyt, S., Isensee, K., Telszewski, M., & Pidgeon, E., (2014). Coastal blue carbon: methods for assessing carbon stocks and emissions factors in mangroves, tidal salt marshes, and seagrasses, *Conservation International, 36* (1), 180

Jones, T., Glass, L., Gandhi, S., Ravaoarinorotsihoarana, L., Carro, A., Benson, L., Ratsimba, H., Giri, C., Randriamanatena, D., & Cripps, G. (2016). Madagascar's mangroves: Quantifying nation-wide and ecosystem specific dynamics, and detailed contemporary mapping of distinct ecosystems. *Remote Sensing, 8* (2), 106

Jones, A., Raja Segaran, R., Clarke, K., Waycott, M., Goh, W., & Gillanders, B. (2020). Estimating mangrove tree biomass and carbon content: a comparison of forest inventory techniques and drone imagery. *Frontiers in Marine Science, 6*, 784

Kaartinen, H., Hyyppä, J., Yu, X., Vastaranta, M., Hyyppä, H., Kukko, A., Holopainen, M., Heipke, C., Hirschmugl, M., Morsdorf, F., & Næsset, E. (2012). An international comparison of individual tree detection and extraction using airborne laser scanning. *Remote Sensing, 4* (4), 950-974

Kauffman, J., & Donato, D. (2012). *Protocols for the measurement, monitoring and reporting of structure, biomass and carbon stocks in mangrove forests*. Working Paper 86. Bogor: CIFOR, p. 40

Kitamura, S., Anwar, C., Chaniago, A., & Baba, S. (1997). *Handbook of Mangroves in Indonesia*. Bali: The International Society for Mangrove Ecosystem, p. 199

Komiyama, A., Ogino, K., Aksornkoae, S., & Sabhasri, S., (1987). Root biomass of a mangrove forest in southern Thailand. 1. Estimation by the trench method and the zonal structure of root biomass. *Journal of Tropical Ecology, 3* (2), 97-108

Komiyama, A., Poungparn, S., & Kato, S., (2005). Common allometric equations for estimating the tree weight of mangroves. *Journal of Tropical Ecology*, 471-477

Larjavaara, M., & Muller-Landau, H. (2013). Measuring tree height: a quantitative comparison of two common field methods in a moist tropical forest. *Methods in Ecology and Evolution, 4* (9), 793-801

Lin, Y., Hyyppä, J., &Jaakkola, A. (2010). Mini-UAV-borne LIDAR for fine-scale mapping. *IEEE Geoscience and Remote Sensing Letters, 8* (3), 426-430

McKee, K., Cahoon, D., & Feller, I., (2007). Caribbean mangroves adjust to rising sea level through biotic controls on change in soil elevation. *Global Ecology and Biogeography, 16* (5), 545-556

Mcleod, E., Chmura, G., Bouillon, S., Salm, R., Björk, M., Duarte, C., Lovelock, C., Schlesinger, W., & Silliman, B. (2011). A blueprint for blue carbon: toward an improved understanding of the role of vegetated coastal habitats in sequestering CO2. *Frontiers in Ecology and the Environment, 9* (10), 552-560

Mitra, A., Sengupta, K., & Banerjee, K. (20 11). Standing biomass and carbon storage of above-ground structures in dominant mangrove trees in the Sundarbans. *Forest Ecology and Management, 261* (7), 1325-1335

Navarro, A., Young, M., Allan, B., Carnell, P., Macreadie, P., & Ierodiaconou, D. (2020). The application of Unmanned Aerial Vehicles (UAVs) to estimate above-ground biomass of mangrove ecosystems. *Remote Sensing of Environment, 242*, 111747

Neukermans, G., Dahdouh-Guebas, F., Kairo, J., & Koedam, N. (2008). Mangrove species and stand mapping in Gazi Bay (Kenya) using Quickbird satellite imagery. *Journal of Spatial Science*, *53* (1), 75-86

Osland, M., Feher, L., Griffith, K., Cavanaugh, K., Enwright, N., Day, R., Stagg, C., Krauss, K., Howard, R., Grace, J., & Rogers, K. (2017). Climatic controls on the global distribution, abundance, and species richness of mangrove forests. *Ecological Monographs*, *87* (2), 341-359

Ouyang, X., & Lee, S. (2020). Improved estimates on global carbon stock and carbon pools in tidal wetlands. *Nature communications*, *11* (1), 1-7

Owers, C., Rogers, K., Mazumder, D., & Woodroffe, C. (2016). Spatial variation in carbon storage: A case study for Currambene Creek, NSW, Australia. *Journal of Coastal Research*, *75*, 1297-1301

Owers, C., Rogers, K., & Woodroffe, C. (2018a). Spatial variation of above-ground carbon storage in temperate coastal wetlands. Estuarine, *Coastal and Shelf Science*, 210, 55-67

Owers, C., Rogers, K. & Woodroffe, C., (2018b). Terrestrial laser scanning to quantify above-ground biomass of structurally complex coastal wetland vegetation. *Estuarine, Coastal and Shelf Science*, *204*, 164-176

Panagiotidis, D., Abdollahnejad, A., Surový, P. & Chiteculo, V. (2017). Determining tree height and crown diameter from high-resolution UAV imagery. *International journal of remote sensing*, *38* (8-10), 2392-2410

Popescu, S. & Wynne, R. (2004). Seeing the trees in the forest. *Photogrammetric Engineering & Remote Sensing*, *70* (5), 589-604

Proisy, C., Couteron, P. & Fromard, F. (2007). Predicting and mapping mangrove biomass from canopy grain analysis using Fourier-based textural ordination of IKONOS images. *Remote Sensing of Environment*, *109* (3), 379-392

Ravindranath, N. & Ostwald, M. (2008). *Carbon Inventory Methods Handbook for Greenhouse Gas Inventory, Carbon Mitigation and Roundwood Production Projects* (pp. 149 – 156). Dordrecht: Springer

Ray, R., Ganguly, D., Chowdhury, C., Dey, M., Das, S., Dutta, M., Mandal, S., Majumder, N., De, T., Mukhopadhyay, S. & Jana, T. (2011). Carbon sequestration and annual increase of carbon stock in a mangrove forest. *Atmospheric Environment*, *45* (28), 5016-5024

Roussel, J., Auty, D., De Boissieu, F. & Meador, A. (2018). lidR: Airborne LiDAR data manipulation and visualization for forestry applications. R package Version 3.0.4

Smith, J., Domke, G., Nichols, M. & Walters, B. (2019). Carbon stocks and stock change on federal forest lands of the United States. *Ecosphere*, *10* (3), 1-17

Soares, M. & Schaeffer-Novelli, Y. (2005). Above-ground biomass of mangrove species. I. Analysis of models. *Estuarine, Coastal and Shelf Science*, *65* (1-2), 1-18

Taillardat, P., Friess, D. & Lupascu, M. (2018). Mangrove blue carbon strategies for climate change mitigation are most effective at the national scale. *Biology letters*, *14* (10), 1-6

Thompson, B., Clubbe, C., Primavera, J., Curnick, D. & Koldewey, H. (2014). Locally assessing the economic viability of blue carbon: A case study from Panay Island, the Philippines. *Ecosystem Services*, *8*, 128-140

Torresan, C., Berton, A., Carotenuto, F., Di Gennaro, S., Gioli, B., Matese, A., Miglietta, F., Vagnoli, C., Zaldei, A. & Wallace, L. (2017). Forestry applications of UAVs in Europe: A review. *International Journal of Remote Sensing*, *38* (8-10), 2427-2447

Turner, I., Harley, M. & Drummond, C. (2016). UAVs for coastal surveying. *Coastal Engineering*, *114*, 19-24

Twilley, R., Chen, R. & Hargis, T. (1992). Carbon sinks in mangroves and theirimplications to carbon budget of tropical coastal ecosystems. *Water, Air, and Soil Pollution*, *64* (1-2), 265-288

Van Vinh, T., Marchand, C., Linh, T., Vinh, D. & Allenbach, M. (2019). Allometric models to estimate above-ground biomass and carbon stocks in *Rhizophora apiculata* tropical managed mangrove forests (Southern Viet Nam). *Forest Ecology and Management*, *434*, 131-141

Wang, L., Gong, P. & Biging, G. (2004). Individual tree-crown delineation and treetop detection in high-spatial-resolution aerial imagery. *Photogrammetric Engineering & Remote Sensing, 70* (3), 351-357

Wannasiri, W., Nagai, M., Honda, K., Santitamnont, P. & Miphokasap, P. (2013). Extraction of mangrove biophysical parameters using airborne LiDAR. *Remote Sensing, 5* (4), 1787-1808

Wicaksono, P. (2017). Mangrove above-ground carbon stock mapping of multi-resolution passive remote-sensing systems. *International Journal of Remote Sensing, 38* (6), 1551- 1578

Wilkes, P., Lau, A., Disney, M., Calders, K., Burt, A., de Tanago, J., Bartholomeus, H., Brede,
B. & Herold, M., (2017). Data acquisition considerations for terrestrial laser scanning of forest plots. *Remote Sensing of Environment, 196*, 140-153

Wylie, L., Sutton-Grier, A. & Moore, A. (2016). Keys to successful blue carbon projects: lessons learned from global case studies. *Marine Policy, 65*, 76-84

Yao, W., Krzystek, P. & Heurich, M. (2012). Tree species classification and estimation of stem volume and DBH based on single tree extraction by exploiting airborne full-waveform LiDAR data. *Remote Sensing of Environment, 123*, 368-380

Yin, D. & Wang, L. (2019). Individual mangrove tree measurement using UAV-based LiDAR data: Possibilities and challenges. *Remote Sensing of Environment, 223*, 34-49

Zhang, W., Qi, J., Wan, P., Wang, H., Xie, D., Wang, X. & Yan, G. (2016). An easy-to-use airborne LiDAR data filtering method based on cloth simulation. *Remote Sensing, 8* (6), p. 501

Zuur, A., Ieno, E. & Elphick, C. (2010). A protocol for data exploration to avoid common statistical problems, *Methods in Ecology and Evolution, 1* (1), 3 – 14